VERSITA

Arch. Min. Sci., Vol. 58 (2013), No 4, p. 1071–1084

Electronic version (in color) of this paper is available: http://mining.archives.pl

DOI 10.2478/amsc-2013-0074

REZA NOURI*, MOHAMMADREZA JAFARI*, MEHRAN ARIAN**, FARANAK FEIZI***, PEYMAN AFZAL***,****

PROSPECTION FOR COPPER MINERALIZATION WITH CONTRIBUTION OF REMOTE SENSING, GEOCHEMICAL AND MINERALOGRAPHICAL DATA IN ABHAR 1:100,000 SHEET, NW IRAN

POSZUKIWANIA ZASOBÓW RUD MIEDZI Z ZASTOSOWANIEM ZDALNYCH TECHNIK WYKORZYSTUJĄCYCH DANE GEOCHEMICZNE I MINERALOGICZNE W POKŁADZIE GEOLOGICZNYM ABHAR 1:100,000 W PÓŁNOCNO-ZACHODNIM IRANIE

Abhar 1:100,000 sheet is located within the Cenozoic Tarom volcano-plutonic belt, NW Iran. The present study is based on the integration of remote sensing techniques on Advanced Spaceborne Thermal Emission and Reflection Radiometer (ASTER), geochemical data analysis consisting of stream sediment and lithogeochemical samples, within geological field observations and mineralographical studies to identify Cu prospect. On ASTER data; using a number of selected methods including band ratio, Least Square Fit (LS-Fit) and Minimum Noise Fraction (MNF) distinguished alternation zones. These methods revealed that three types of alterations: argillic, phyllic, and iron oxide zones occurring at the NE and SE of Abhar sheet, while the propylitic and silica zones are developed in NW and SW of the studied area. Lineaments were identified by aid of false color composite, high pass filters and hill-shade DEM techniques that two NW-SE and NE-SW major trends were determined. Geochemical anomalies were separated by number–size (N-S) method. Interpretation of N-S log–log plots of Cu in the area may be a result of the three steps of enrichment, i.e., mineralization and later dispersions. Field checks and Mineralgraphical studies also confirm the existence of suitable copper mineralization.

Keywords: Alteration zones, ASTER, Geochemical data, Abhar, Iran

Pokład geologiczny Abhar 1:100,100 zlokalizowany jest w obrębie kenozoicznego pasa skał magmowych pochodzenia wulkanicznego Tarom w północno-zachodnim Iranie. W pracy przedstawiono połączenie zastosowań metod zdalnych wykorzystujących technologię ASTER (Advanced Spaceborne Thermal Emission and Refelection Radiometer), analizę danych geochemicznych zebranych na podstawie osadów dennych ze strumieni oraz próbek skał w obrębie pola obserwacji a także danych mineralogicznych w celu rozpoznania skupisk rud miedzi. Na podstawie danych uzyskanych przy użyciu technologii

* DEPARTMENT OF GEOLOGY, NORTH TEHRAN BRANCH, ISLAMIC AZAD UNIVERSITY, TEHRAN, E-MAIL: reza_noor2002@yahoo.com
** DEPARTMENT OF GEOLOGY, SCIENCE AND RESEARCH BRANCH, ISLAMIC AZAD UNIVERSITY, TEHRAN, IRAN
*** DEPATMENT OF MINING ENGINEERING, SOUTH TEHRAN BRANCH, ISLAMIC AZAD UNIVERSITY, TEHRAN, IRAN
**** CAMBORNE SCHOOL OF MINES, UNIVERSITY OF MINES, UNIVERSITY OF EXETER, PENRYN, UK

ASTER i poddanych obróbce przy użyciu różnorodnych technik: badanie układu pasm, dopasowanie metodę najmniejszych kwadratów oraz minimalny współczynnik szumów, rozróżniono strefy przeobrażeń skał. Metody te pozwoliły na wykrycie trzech typów skał przeobrażonych: gliniaste, łupki ilasto-mikowe oraz strefy występowania tlenków żelaza występujące na północno-wschodnich (NE) i południowo-zachodnich (NW) krańcach pasa Abhar. W części północno-zachodnie (NW) i południowo-zachodniej (SW) badanego obszaru stwierdzono występowanie stref propilitu i krzemianów. Lineacje wykryto przy pomocy metody badania zakresu barw, filtrów wysoko-przepustowych, techniki określania wysokości, na tej podstawie określono dwa główne trendy: NW-SE oraz NE-SW. Anomalie geologiczne wydzielono za pomocą metody N-S (liczba-wymiar). Interpretacja wykresów N-S wykonanych w skali logarytmicznej wykazała, że zaobserwowany układ może być wynikiem trzech etapów wzbogacania: mineralizacji i późniejszego rozproszenia. Badania terenowe oraz analizy mineralograficzne potwierdzają obecność odpowiednio zmineralizowanej miedzi.

Słowa kluczowe: strefy przeobrażeń skał, technologia ASTER, dane geochemiczne, pokład geologiczny Abhar, Iran

1. Introduction

Iran is located in the Alpine-Himalian orogenic and metalogenic belt and has high potentials for gold, copper and other base metal deposits that many Iranian geologist researchers have been used satellite images for exploration purposes and recognizing hydrothermally altered rocks (Asadi Haroni & Lavafan, 2007; Azizi et al., 2010; Beiranvand Pour & Hashim, 2012). For instance, Moghtaderi et al., (2007) separated some alkali metasomatose in the Chadourmalou district in the vicinity of iron ore deposits in the NW Iran; remote sensing methods are using for distinguished different alteration zones in the different magmatic arcs and belts of Iran (Mars & Rowan, 2006; Poormirzaee & Mohammady Oskouei, 2010; Beiranvand Pour et al., 2011; Oskouei & Busch, 2012). Separation of anomalies and background is the most important aim of geochemical exploration operations especially for metallic deposits. Stream sediment and lithogeochemical studies are essential for prospecting of different ore deposits (Hawkes & Webb, 1979). Several methods are used for geochemical data interpretation and modelling such as classical statistics (e.g., Tukey, 1977; Hawkes & Webb, 1979; Reimann et al., 2005), fractal and multifractal modelling (Cheng et al., 1994; Agterberg et al., 1996; Cheng, 1999; Li et al., 2003; Zuo et al., 2009; Afzal et al., 2010a; Afzal et al., 2010b) and singularity modelling (Cheng, 2007). Fractal theory has been established by Mandelbrot (1983) as an important non-Euclidean branch in geometry. Several methods have been proposed and developed based on fractal geometry for application in geosciences since the 1980s (Agterberg et al., 1993; Sanderson et al., 1994; Cheng, 1999; Turcotte, 1997, 2002; Goncalves et al., 2001; Monecke et al., 2005; Gumiel et al., 2010; Afzal et al., 2010b; Zuo, 2011; Sadeghi et al., 2012). The present study is based on the integration of remote sensing techniques and geochemical data analysis (stream sediment and lithogeochemical samples), as well as geological field verification and mineralographical studies to identify Cu prospects in the Abhar 1:100,000 sheet, NW Iran.

2. Geological setting of the Abhar 1:100,000 sheet

Abhar 1:100,000 sheet is located in Zanjan province (NW Iran) which is part of Tarom polymetallic zone (Fig. 1). Tarom polymetallic Zone is a part of west Alborz mountain range that in Eocene epoch has been formed by mainly volcanic rocks eruption. Rock sequences are equivalent of Karaj formation and associated with volcanic lavas of basalt, andesite, basaltic andesite and trachyte that are all intruded by Oligocene intrusive bodies (Hirayama et al., 1966). Large mass magmatic outcrops have been occurred in Abhar sheet with alkali granite, granite, granodiorite, quartz monzonite, quartz monzodiorite, quartz syenite. Magmatic activities in area have been issued by tectonic activities including orogeny phases. Certainly Pyrenean orogeny is effective action in occurring of Eocene-Oligocene intrusive igneous rocks in the area (Mousavi, 2012). There are several metallic deposits and mines in terms of copper, gold, Pb-Zn and Iron ores.

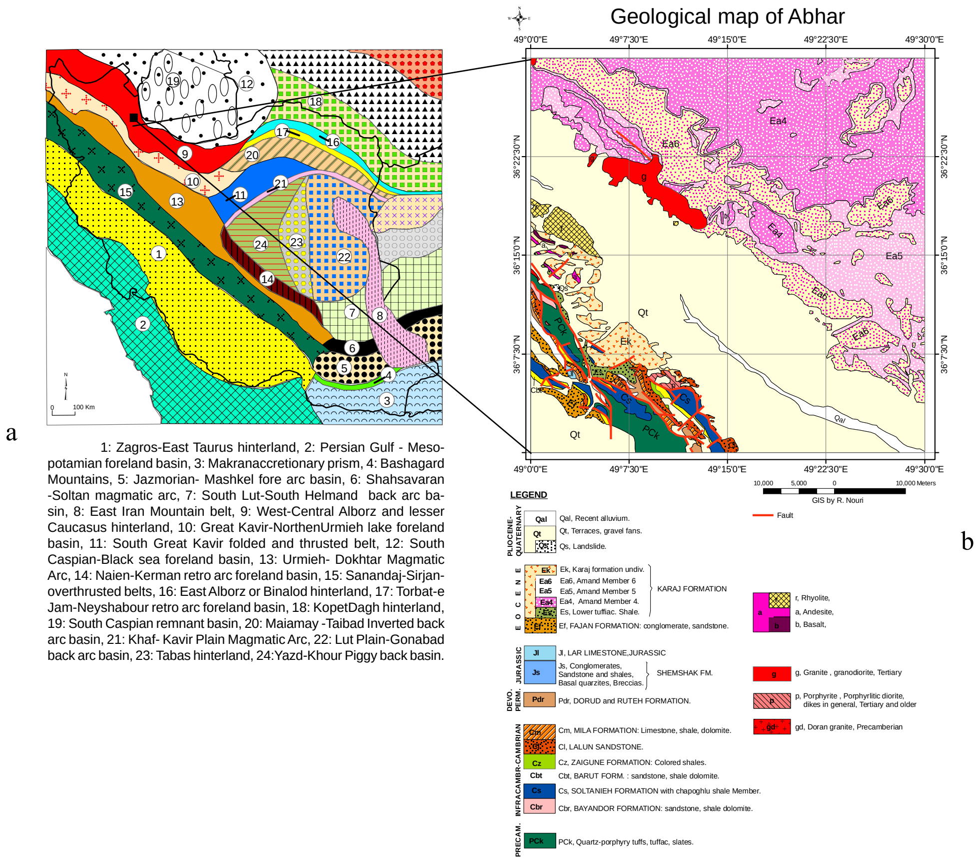

Fig. 1. a – Generalized geology map of Iran (Arian, 2011) The study area is shown in the square box. b – Geological map of studied area based on 1:1250000 geological map of Zanjan

3. Materials and methods

The aims of the paper are to perform Least Square Fit (LS-Fit), Minimum Noise Fraction (MNF) and band ratio to map zones of hydrothermal alteration on the ASTER (Advanced Spaceborne Thermal Emission and Reflection Radiometer) satellite imagery data and delineation of high intensive copper anomalies using Number–Size (N-S) fractal method based on stream sediments and lithogeochemical data for finding new prospects in copper mineralization in Abhar 1:100,000 sheet. ENVI and ArcGIS software packages were used for multi-spectral image interpretation and fractal modeling of geochemical data, respectively.

4. Result and discussion

4.1. Remote sensing interpretation

The ASTER is an advanced optical sensor comprised of 14 spectral channels that will provide scientific and also practical data regarding various field related to the study of the earth (Rowan & Mars, 2003; Moghtaderi et al., 2007; Yousefifar et al., 2011). Numerous factors affect the signal measured at the sensor, such as drift of the sensor radiometric calibration, atmospheric and topographical effects. Therefore, data set AST_L1B_010_82007451101083113331 in hierarchical data format (HDF) was used and radiance correlation such as wavelength, dark subtract and log residual by ENVI4.4 software which is essential for multispectral images, were employed.

4.1.1. Hydrothermal alteration zones′ investigation

Many image analysis and processing techniques can be used to interpret the remote sensing spectral data (Mars & Rowan, 2006; Azizi et al., 2010; Poormirzaee & Mohammady Oskouei, 2010; Beiranvnd Pour & Hashim, 2012; Oskouei & Busch, 2012). In this research, band ratio, Least Square Fit (LS-Fit) and Minimum Noise Fraction (MNF) methods were used on ASTER data for discrimination of alteration zones.

Band ratio

Band ratio is a technique where the digital number (DN) value of one band is divided by the DN value of another band. BRs can be useful for highlighting certain features or materials that cannot be seen in the raw bands. Similarly, the choice of bands depends on their spectral reflectance and positions of the absorption bands of the mineral being mapped (Inzana et al., 2003; Kujjo, 2010; Rajendran et al., 2012). For instance, to enhance a specific alteration mineral that hosts a distinct absorption feature, the most unique spectral ratio for that mineral is employed. In order to discrimination of iron oxide, argillic, phyllic, propylitic and silica ratios (3/1), (5×7/6×6), (7/6), (6+9/7+8) and (13/12) were used (Fig. 2).

Least Squares Fitting (LS-Fit)

The technique assumes that the bands used as input values are behaving as the variables of a linear expression and the ‘y’ value of the equation, namely the predicted band information, gives us a calculated output value. This predicted band is what that band should be according to the linear equation. The minerals which are sensitive to a specific band are then differentiated from the features which are reflective to the other bands as well; just by taking the difference between the predicted values and the original values (Yetkin et al., 2004). Distribution of iron oxide was created by using all the 3 visible and near-infrared (VNIR) bands as the input bands and VNIR-b3 as the modelled band. Also, argillic, phyllic and propylitic alterations were mapped by using residual band SWIR-b3, residual band SWIR-b2 and residual SWIR-b5. Moreover, silica zone was mapped by using residual band TIR-b3 (Fig. 3).

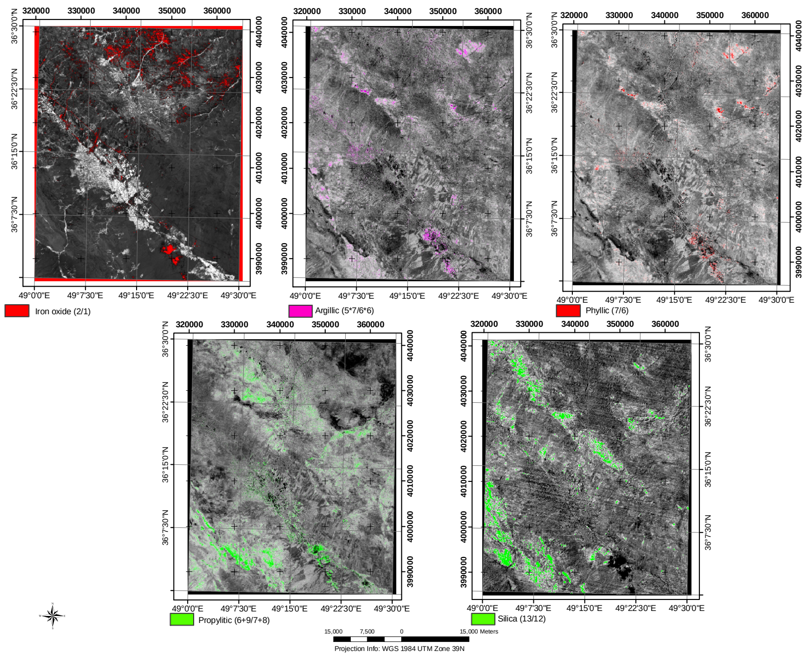

Fig. 2. The iron oxide, argillic, phyllic, propylitic and silica images prepared based on band ratio method

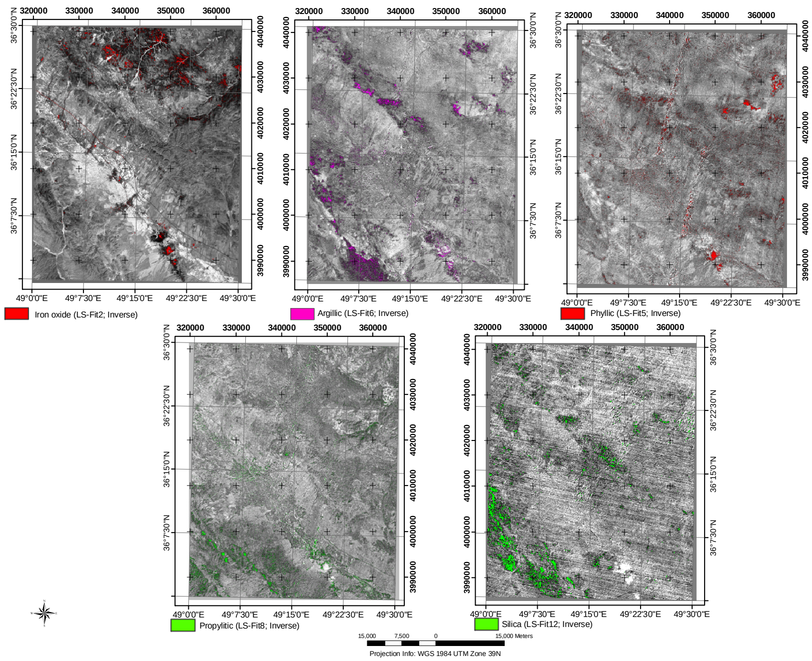

Fig. 3. The iron oxide, argillic, phyllic, propylitic and silica images prepared based on LS-Fit method

Minimum Noise Fraction

The Minimum Noise Fraction (MNF) analysis can identify the locations of spectral signature anomalies. This process is of interest to exploration geologist because spectral anomalies are often indicative of alterations due to hydrothermal mineralization. MNF involves two steps; in first step which is also called noise whitening, principal components for noise covariance matrix are calculated. This step decorrelates and rescales the noise in the data. In second step principal components are derived from the noise whitened data. The data can then be divided into two parts. One part associated with large Eigen values and the other part with near unity Eigen values and noise dominated images. Using data with large Eigen values separates the noise from the data, and improves spectral results (Beiranvnd Pour et al., 2011). MNF bands 2, 7, 5, 8 and 11 were used for iron oxide, argillic, phyllic, propylitic and silica alterations (Fig. 4).

Three types of alterations including argillic, phyllic, and iron oxide zones occurring at the NE and SE of Abhar 1:100,000 sheet, while the propylitic and silica zones are existed in the NW and SW parts of the studied area that all method accordance to each other.

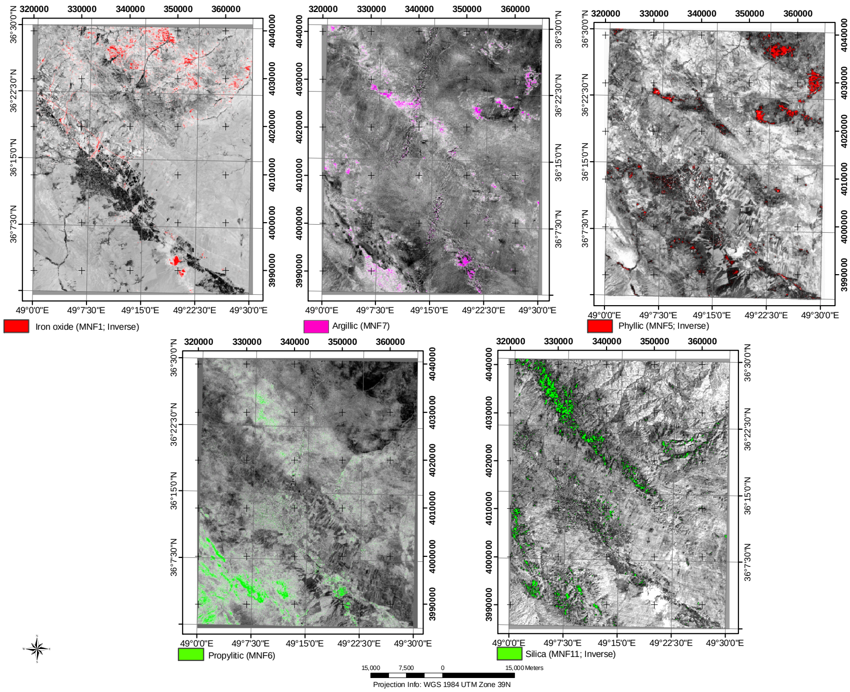

Fig. 4. The iron oxide, argillic, phyllic, propylitic and silica images prepared based on MNF method

4.1.2. Lineament extraction

The lineaments usually appear as straight lines or "edges" on the satellite images which in all cases contributed by the tonal differences within the surface material. The knowledge and the experience of the user is the key point in the identification of the lineaments particularly to connect broken segments into a longer lineament (Sarp, 2005; Abarca, 2006; Weldemariam, 2009). Therefore, different combinations of three bands are examined and the best visual quality is obtained with a false color image utilizing three 7, 4, and 2 (in blue, green and red respectively). Moreover, filtering operations are used to emphasize or deemphasize spatial frequency in the image. The filtering operation will sharpen the boundary that exists between adjacent units. Standard GIS techniques have been carried out to help in the evaluation of the lineaments detected. Furthermore, hill-shade Digital Elevation Model (DEM) technique is effective in creating images that enhance geomorphologic features. Therefore, Hill-shades DEM with different azimuth direction and sun angle were used in this study and two NW-SE and NE-SE major trends were determined for structural features (Fig. 5).

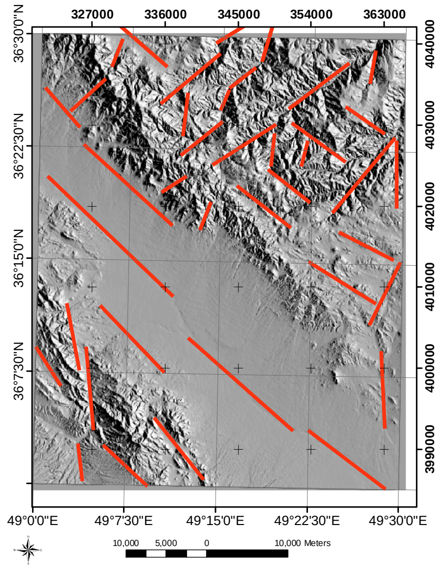

a

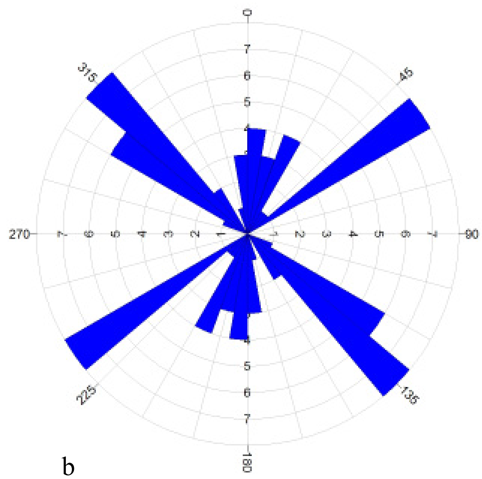

b

Fig. 5. a – Lineament of studied area based on shaded relief. b – Rose diagram of studied area

4.2. Geochemical data analysis

In the studied area, 1131 stream sediment samples were collected for first stage of geochemical exploration and also, 121 lithogeochemical samples were collected from the area (Fig. 6). The samples were chemical analyzed by ICP-MS method for 42 elements especially for copper and gold. In this study, Number-Size (N-S) fractal method was utilized for High intensive Cu anomalies in the Abhar 1:100,000 sheet.

4.2.1. Number-Size fractal method

The Number–Size (N-S) method, which was originally proposed by Mandelbrot (1983), can be used to describe the distribution of geochemical populations without pre-processing of

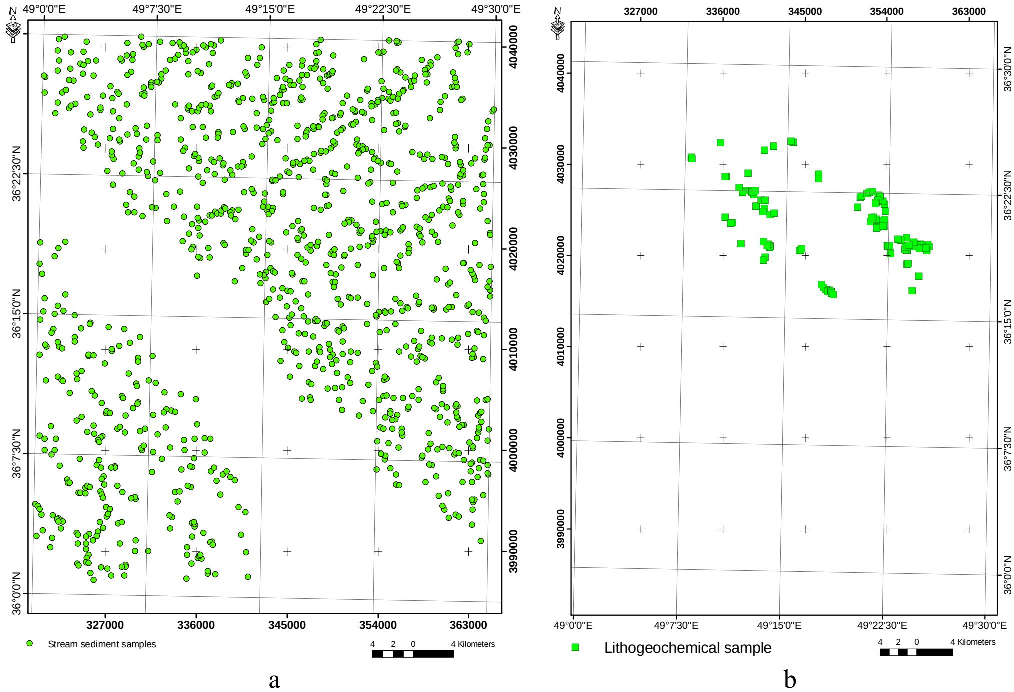

Fig. 6. a – Stream sediment. b – Lithogeochemical samples location map of the Abhar sheet

data. The method indicates that there is a relationship between desirable attributes (e.g., ore elements) and their cumulative numbers of samples. Based on the model, Agterberg (1995) proposed a multifractal model named size-grade for determination of the spatial distributions of giant and super-giant ore deposits. Monecke et al., (2005) used the N–S fractal model to characterize element enrichments associated with metasomatic processes during the formation of hydrothermal ores in the Waterloo massive sulfide deposit, Australia. A power-law frequency model has been proposed to describe the N–S relationship according to the frequency distribution of element concentrations and cumulative number of samples with those attributes (Li et al., 1994; Sanderson et al., 1994; Shi & Wang, 1998; Turcotte, 1996; Zuo et al., 2009). The model is expressed by the following equation (Mandelbrot, 1983; Deng et al,. 2010):

$$N(\geq\rho) = F\rho^{-D} \tag{1}$$

where ρ denotes element concentration, $N(\geq\rho)$ denotes cumulative number of samples with concentration values greater than or equal to ρ, F is a constant and D is the scaling exponent or fractal dimension of the distribution of element concentrations. According to Mandelbrot (1983) and Deng et al., (2010), log–log plots of $N(\geq\rho)$ versus ρ show straight line segments with different slopes $-D$ corresponding to different concentration intervals.

4.2.2 Stream sediment data analysis

Stream sediment geochemistry was found to be an efficient method for outlining potentially mineralized areas. Finer (silt) fractions of alluvial sediments represent well the geochemistry of the drainage pattern and also reduce a “nugget effect” during sampling (Fletcher, 1997; Aichler et al., 2008). This method can be effectively used also in regional prospection for gold as shown by Xie & Wang (1991). The analyzed grades in all samples were sorted based on decreasing grades and cumulative numbers were calculated for grades. Finally, log–log plot was generated for Cu (Fig. 7). Break points between straight-line segments in the log–log plot show threshold values separating populations of geochemical concentration values representing geological differences due to distinct geochemical processes. Elemental geochemical populations are demonstrated in this log–log plot. On the basis of this process, there are four populations for Cu that the high intensive Cu anomalies have values more than 112.2 ppm. The area was gridded to 184×184 m^2 cells for Cu values interpolation. The interpolation method is Inverse Distance Squared (IDS) was used for generation of Cu distribution map. The high values of Cu (≥112 ppm) were located in central, NE and northern parts of the Abhar sheet, as depicted in Fig.7.

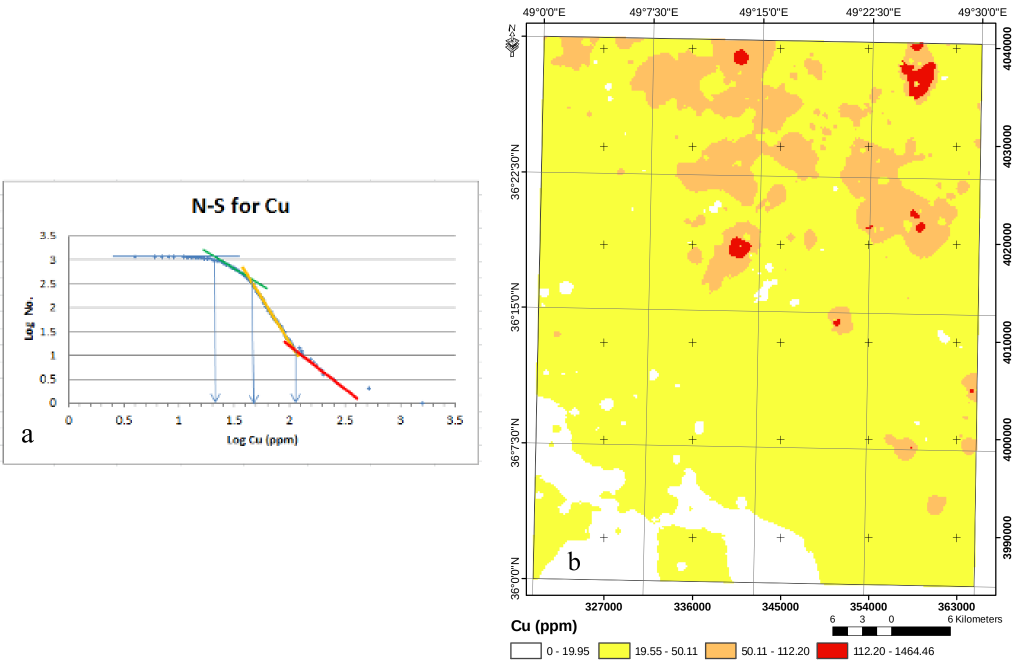

Fig. 7. a – Log–log plots from C–N method for Cu. b – Cu stream sediment population distribution map based on the C–N method

4.2.3. Lithogeochemistry

After analysis of stream sediment data, lithogeochemical samples were collected from anomalous parts in central and northern parts of the area (Fig. 6). The N-S log–log plot for Cu show there are four geochemical populations, as shown in Fig. 8. Extreme intensity Cu anomaly is started from 6.3% Cu and located in central parts of the Abhar sheet. Additionally, anomalous parts derived via stream sediments and lithogeochemcal data in centre of the area were correlated. High intensive Cu anomalies (1.6-6.3%) were situated in the central and northern parts of the area (Fig. 8). Integration of remote sensing and geochemical data is shown in Fig. 9.

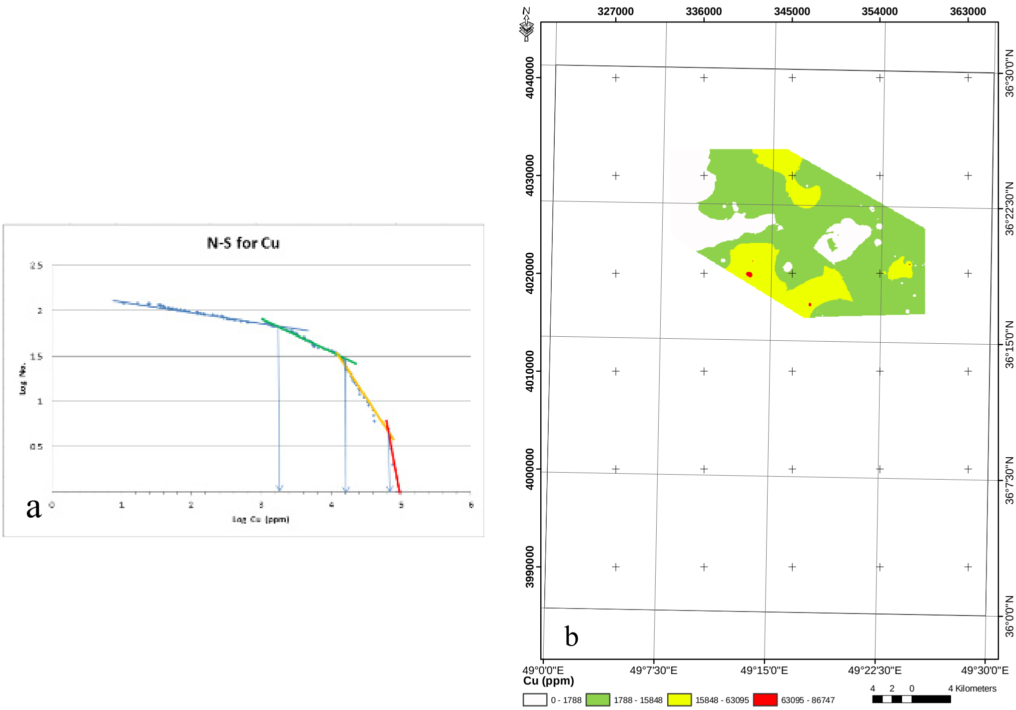

Fig. 8. a – Log–log plots from C–N method for Cu. b – Cu lithogeochemical population distribution map based on the C–N method

4.3. Ground –truth verification and ore mineralographical study

To evaluate the ASTER satellite data and discriminate geochemical anomalies, field-geological observations have been validated. In almost all cases, field studies confirmed in showing real alteration zones and detection of area Cu mineralization by interpreted of remote sensing imagery and high intensive Cu geochemical anomalies (Fig. 9). In the field, alteration zones revealed by different band ratios, LS-Fit and MNF methods of the satellite data are well correlated with Cu mineralization that confirmed by N-S fractal method. The mineralogical as-

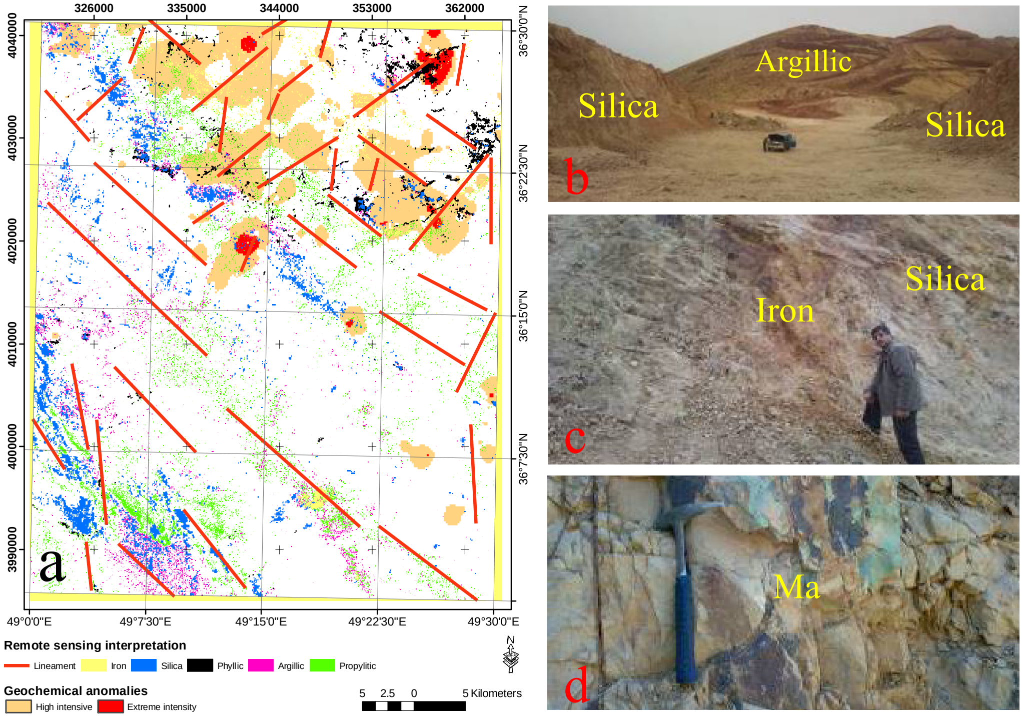

Fig. 9. a – Integration of remote sensing and geochemical data in the Abhar sheet. b – Regional view of alteration in the studied area. c – Iron oxide and silica rocks. d – Malachite (Ma) mineralization

semblages of the copper such as borniteand malachite were determined in the thin and polish sections. Chalcopyrite which are sometimes altered to magnetite and other iron oxides were also distinguished that illustration in Fig. 10.

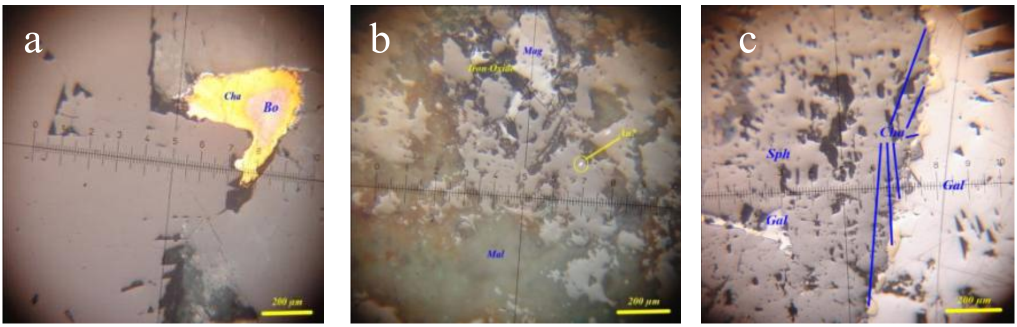

Fig. 10. Results obtained by mineralographical studies in the Abhar area a – Assemblage of Chalcopyrite and bornite.. b – Magnetite with other iron oxides, malachite and gold particle. c – Society of copper and Zn-Pb mineralization which are chalcopyrite, galena and sphalerite

5. Conclusions

The use of ASTER data in the early stages of mineral exploration was very successful for recognition of the hydrothermal alterations. Moreover, ASTER multi-spectral images could be used for the identification of lineaments possibly related to faults. The performance of conventional image processing techniques such as band ratio, LS-Fit and MNF has been evaluated on ASTER bands. Results show that the integration of the image processing techniques has great ability to detect iron oxide, argillic, phyllic, propylitic and silica zones.

Separation of geochemical anomalies based on stream sediments and lithogeochemical data are important for finding of ore element prospects. Results obtained by the study show those fractal methods, especially N-S, are useful tools for delineation of high intensive geochemical anomalies from low intensity anomalous parts and background. Interpretation of N-S log–log plots of Cu in the area indicates that the three steps of enrichment, i.e., mineralization and later dispersions occurred in the Abhar sheet. Field geological observations also confirmed that Cu anomalies have direct relationships with the faults especially in the north to central parts of the area in the Abhar sheet. Furthermore, there is a good correlation between phyllic, argillic, propylitic and silica alteration zones and anomalous concentration of Cu. Mineralgraphical studies also confirm the existence of new copper prospects in central and NE parts of the area.

Acknowledgment

The authors are grateful to Mr. Beighi and Mr. Haghigat, Exploration Department of Zanjan Province Industry, Mine and Trade Organization of Iran and KanAzin Consulting Engineering Company for their sincere help and valuable discussions especially in field checks and interpretation of microscopic sections.

References

Abarca M.A.A., 2006. *Lineament extraction from digital terrain models*. Master of Science dissertation, Addis Ababa University, 1-81 pp.

Afzal P., Fadakar Alighalandis Y., Khakzad A., Moarefvand P., Rashidnejad Omran N., 2010a. *Application of power spectrum-area fractal model to separate anomalies from background in Kahang Cu-Mo porphyry deposit, Central Iran*. Arch. Min. Sci., Vol. 56, No. 3, p. 389-401.

Afzal P., Khakzad A., Moarefvand P., Rashidnejad Omran N., Esfandiari B., Fadakar Alghalandis Y., 2010b. *Geochemical anomaly separation by multifractal modeling in Kahang (Gor Gor) porphyry system, Central Iran*. J Geochem Explor 104, 34-46.

Agterberg F.P., Cheng Q., Wright D.F., 1993. *Fractal modeling of mineral deposits*. In: Elbrond, J., Tang, X. (Eds.), 24th APCOM symposium proceeding, Montreal, Canada, 43-53 pp.

Agterberg F.P., 1995. *Multifractal modeling of the sizes and grades of giant and supergiant deposits*. International Geology Review 37, 1-8.

Agterberg F.P., Cheng Q. Brown A., Good D., 1996. *Multifractal modeling of fractures in the Lac du Bonnet Batholith, Manitoba*. Comput Geosci 22(5). 497-507.

Aichler J., Malec J., Večeřa J., Hanžl P., Buriánek D., Sidorinová T., Táborský Z., Bolormaa K., Byambasuren D., 2008. *Prospection for gold and new occurrences of gold-bearing mineralization in the eastern Mongolian Altay*. Journal of Geosciences, 53 (2), 123-138.

Arian M., 2011. *Basement Tectonics and Geology of Iran*. Asar Nafis Press, Tehran, p. 140-147 (In Persian).

Asadi Haroni H., Lavafan A., 2007. *Integrated Analysis of ASTER and Landsat ETM Data to Map Exploration Targets in the Muteh Gold -Mining Area, IRAN*. 5th International Symposium on Spatial Data Quality, Enschede, The Netherlands.

Azizi H., Tarverdi M.A., Akbarpour A., 2010. *Extraction of hydrothermal alterations from ASTER SWIR data from east Zanjan, northern Iran*. Advances in Space Research 46, 99-109.

Beiranvand Pour A., Hashim M., Marghany M., 2011. *Using spectral mapping techniques on short wave infrared bands of ASTER remote sensing data for alteration mineral mapping in SE Iran*. International Journal of the Physical Sciences 6(4), 917-929.

Beiranvand Pour A., Hashim M., 2012. *The application of ASTER remote sensing data to porphyry copper and epithermal gold deposits*. Ore Geology Reviews 44, 1-9.

Cheng Q., Agterberg F.P., Ballantyne S.B., 1994. *The separation of geochemical anomalies from background by fractalmethods*. Journal of Geochemical Exploration 51, 109-130.

Cheng Q., 1999. *Spatial and scaling modelling for geochemical anomaly separation*. J Geochem Explor 65(3), 175-194.

Cheng Q., 2007. *Mapping singularities with stream sediment geochemical data for prediction of undiscovered mineral deposits in Gejiu, Yunnan Province, China*. Ore Geology Reviews 32, 314-324.

Deng J., Wang Q., Yang L., Wang Y., Gong Q., Liu H., 2010. *Delineation and explanation of geochemical anomalies using fractal models in the Heqing area, Yunnan Province, China*. Journal of Geochemical Exploration 105, 95-105.

Fletcher W.K., 1997. *Stream sediment geochemistry in today's exploration world*. In: Proceeding of exploration 97: Fourth Decennial Internation Conference on Mineral exploration, Gubins, A.G., Editor, 249-260 pp.

Goncalves M.A., Mateus A., Oliveira V., 2001. *Geochemical anomaly separation by multifractal modeling*. J. Geochem. Explor. 72, 91-114.

Gumiel P., Sanderson D.J., Arias M., Roberts S., Martín-Izard A., 2010. *Analysis of the fractal clustering of ore deposits in the Spanish Iberian Pyrite Belt*. Ore Geology Reviews 38, 307-318.

Hawkes R.A.W., Webb H.E., 1979. *Geochemistry in mineral exploration, 2nd edn*. Academic Press, New York, 657 pp.

Hirayama K., Haghipour A., Hajian J., 1966. *Geological map of Zanjan*. Geological Survey of Iran (GSI).

Inzana J., Kusky T., Higgs G., Tucker R., 2003. *Supervised classifications of Landsat TM band ratio images and Landsat TM band ratio image with radar for geological interpretations of central Madagascar*. Journal of African Earth Sciences 37, 59-72.

Kujjo C.P., 2010. *Application of remote sensing for gold exploration in the Nuba Montains, Sudan*. Bowling Green State University, Master of Science Thesis, 99 pp.

Li C., Xu Y., Jiang X., 1994. *The fractal model of mineral deposits*. Geology of Zhejiang 10, 25-32 (In Chinese with English Abstract).

Li C., Ma T., Shi J., 2003. *Application of a fractal method relating concentrations and distances for separation of geochemical anomalies from background*. J. Geochem. Explor. 77, 167-175.

Mandelbrot B.B., 1983. *The fractal geometry of nature*. Freeman, San Fransisco, 1-468 pp.

Mars J.C., Rowan L.C., 2006. *Radiometer (ASTER) data and logical operator algorithms arc, Iran, using Advanced Spaceborne Thermal Emission and Reflection Regional mapping of phyllic and argillic altered rocks in the Zagros magmatic*. Geosphere 2, 161-186.

Moghtaderi A., Moore F., Mohammadzadeh A., 2007. *The application of advanced space-borne thermal emission and reflection (ASTER) radiometer data in the detection of alteration in the Chadormalu paleocrater, Bafq region, Central Iran*. Journal of Asian Earth Sciences 30: 238-252.

Monecke T., Monecke J., Herzig P.M., Gemmell J.B., Monch W., 2005. *Truncated fractal frequency distribution of element abundance data: a dynamic model for the metasomatic enrichment of base and precious metals*. Earth and Planetary Science Letters 232, 363-378.

Mousavi S.R., 2012. *Theory and modified rules to determine uncertainty in mineral prospection*. PhD dissertation, TU Clausthal 1-120 pp.

Oskouei M., Busch W., 2012. *A selective combined classification algorithm for mapping alterations on ASTER data*. Appl. Geomat. 4, 47-54.

Poormirzaee R., Mohammady Oskouei M., 2010. *Use of spectral analysis for detection of alterations in ETM data, Yazd, Iran*. Applied Geomatics 2, 147-154.

Rajendran S., Khirbash S.A., Pracejus B., Nasir S., Al-Abri A.H., Kusky T.M., Ghulam A., 2012. *ASTER detection of chromite bearing mineralized zones in Semail Ophiolite Massifs of the northern Oman Mountains: Exploration strateg*. Ore Geology Reviews 44, 121-135.

Reimann C., Filzmoser P., Garrett R.G., 2005. *Background and threshold: critical comparison of methods of determination*. Science of the Total Environment 346, 1-16.

Rowan L.C., Mars J.C., 2003. *Lithologic mapping in the Mountain Pass, California area using Advanced Spaceborne Thermal Emission and Reflection Radiometer (ASTER) data*. Remote Sensing of Environment 84, 350-366.

Sadeghi B., Moarefvand P., Afzal P., Yasrebi A.B., Daneshvar Saein L., 2012. *Application of fractal models to outline mineralized zones in the Zaghia iron ore deposit, Central Iran*. Journal of Geochemical Exploration 122, 9-19.

Sanderson D.J., Roberts S., Gumiel P., 1994. *A fractal relationship between vein thickness and gold grade in drill core from La Codosera, Spain*. Econ Geol 89, 168-173.

Sarp G., 2005. *Lineament Analysis from Satellite Images, North-West of Ankara*. Master of Science Dissertation, School of Natural and Applied Science of Middle East Technical University.

Shi J., Wang C., 1998. *Fractal analysis of gold deposits in China: implication for giant deposit exploration*. Earth Sci. J. China Univ. Geosci. 23:616-618 (In Chinese with English Abstract).

Tukey J.W., 1977. *Exploratory Data Analysis*. First ed. Pearson, pp 1-688.

Turcotte D.L., 1996. *Fractals and Chaos in Geophysics, second ed*. Cambridge University Press, Cambridge UK, 81-99 pp.

Turcotte D.L., 1997. *Fractals and chaos in geology and geophysics*. Cambridge Univ., Press, Cambridge.

Turcotte D.L., 2002. *Fractals in petrology*. Lithos 65, 261-271.

Weldemariam A.F., 2009. *Mapping Hydrothermally Altered Rocks and Lineament Analysis Through Digital Enhancement of ASTER Data Case Study: Kemashi area, Western Ethiopia*. Master of Science dissertation, Addis Ababa University, 79 pp.

Xie X., Wang X., 1991. *Geochemical exploration for gold: a new approach to an old problem*. J. Geochem. Explor., 40, 25-48.

Yetkin E., Toprak V., Suezen M.L., 2004. *Alteration Mapping By Remote Sensing: Application To Hasandağ-Melendiz Volcanic, Complex*. Geo-Imagery Bridging Continents XXth ISPRS Congress, Istanbul.

Yousefifar S., Khakzad A., Asadi Harooni H., Karami J., Jafari M.R., Vosoughi Abedin M., 2011. *Prospection of Au and Cu bearing targets by exploration data combination in southern part of Dalli Cu-Au porphyry deposit, Central Iran*. Arch. Min. Sci., Vol.. 56, No. 1, p. 21-34.

Zuo R., Cheng Q., Xia Q., 2009. *Application of fractal models to characterization of vertical distribution of geochemical element concentration*. J. Geochem. Explor. 102(1), 37-43.

Zuo R., 2011. *Identifying geochemical anomalies associated with Cu and Pb-Zn skarn mineralization using principal component analysis and spectrum-area fractal modeling in the Gangdese Belt, Tibet (China)*. Journal of Geochemical Exploration 111, 13-22.

Received: 10 January 2013